A Porcine Anterior Segment Perfusion and Transduction Model With Direct Visualization of the Trabecular Meshwork

Ralitsa T. Loewen,[1] Pritha Roy,[1] Daniel B. Park,[1] Adrianna Jensen,[1] Gordon Scott,[1] Devora Cohen-Karni,[1] Michael P. Fautsch,[2] Joel S. Schuman,[1] and Nils A. Loewen[1]

[1]Department of Ophthalmology, University of Pittsburgh, Pittsburgh, Pennsylvania, United States
[2]Department of Ophthalmology, Mayo Clinic, Rochester, Minnesota, United States

Correspondence: Nils A. Loewen, Department of Ophthalmology, University of Pittsburgh, 203 Lothrop, Suite 819, Pittsburgh, PA 15213, USA;
loewen.nils@gmail.com.

Submitted: September 5, 2015
Accepted: February 13, 2016

Citation: Loewen RT, Roy P, Park DB, et al. A porcine anterior segment perfusion and transduction model with direct visualization of the trabecular meshwork. *Invest Ophthalmol Vis Sci*. 2016;57:1338–1344. DOI:10.1167/iovs.15-18125

Purpose. To establish a consistent and affordable, high quality porcine anterior segment perfusion and transduction model that allows direct visualization of the trabecular meshwork.

Methods. Porcine anterior segments were cultured within 2 hours of death by removing lens and uvea and securing in a specially designed petri dish with a thin bottom to allow direct visualization of the trabecular meshwork with minimal distortion. Twenty-two control eyes (CO) with a constant flow rate were compared to eight gravity perfused eyes (CO_{gr}, 15 mm Hg). We established gene delivery to the TM using eGFP expressing feline immunodeficiency virus (FIV) vector GINSIN at 10^8 transducing units (TU) per eye (GINSIN_8, $n = 8$) and 10^7 TU (GINSIN_7, $n = 8$). Expression was assessed for 14 days before histology was obtained.

Results. Pig eyes were a reliable source for consistent and high quality anterior segment cultures with a low failure rate of 12%. Control eyes had an intraocular pressure (IOP) of 15.8 ± 1.9 mm Hg at fixed pump perfusion with 3 μL/min compared to gravity perfused CO_{gr} with imputed 3.7 ± 1.6 μL/min. Vector GINSIN_8 eyes experienced a transient posttransduction IOP increase of 44% that resolved at 48 hours; this was not observed in GINSIN_7 eyes. Expression was higher in GINSIN_8 than in GINSIN_7 eyes. Trabecular meshwork architecture was well preserved.

Conclusions. Compared with previously used human donor eyes, this inexpensive porcine anterior segment perfusion model is of sufficient, repeatable high quality to develop strategies of TM bioengineering. Trabecular meshwork could be observed directly. Despite significant anatomic differences, effects of transduction replicate the main aspects of previously explored human, feline and rodent models.

Keywords: porcine eyes, trabecular meshwork, glaucoma, lentiviral transduction, eGFP

The cost and availability of consistently high quality human donor eyes are a significant impediment to research involving both the engineering of aqueous humor outflow and hypothesized trabecular meshwork (TM) stem cells. This is becoming more pertinent as the prevalence of glaucoma continues to rise.[1]

In search for readily available model systems, investigators have explored other species. The common house cat has a more diffuse drainage system with a spread out plexus that is not able to provide sufficient outflow resistance even when a feline myocilin mutant that has an aggressive childhood phenotype in humans is overexpressed.[2] Rodent models have the advantage of cost containment in in vivo experimentation and well-developed molecular biology tools. However, while mice and rats share a circular drainage structure similar to the human Schlemm's canal, their lacy TM has only 3 to 10 layers on thin trabeculae. Nonhuman primates have an outflow tract that is nearly indistinguishable from that of humans, but their husbandry is very demanding and expensive. The outflow tract of pig eyes has been described as sharing many similarities with primate eyes that are lacking in other nonprimate eyes.[3] Most notably, it has a relatively large, wedge-shaped TM and circumferential drainage elements that are analogous to discontinuous Schlemm's canal segments,[4] commonly referred to as the angular aqueous plexus.[5] Features include human biochemical glaucoma markers[4] and microphysiological properties such as giant vacuole formation by the endothelium of Schlemm's canal.[3] The recently sequenced genome of *Sus scrofa* indicates that pigs and humans have a closer genome match than mice and humans[6–8] for instance, which may provide new tools for a porcine glaucoma model. Because of these advantages and the increased interest in using pig eyes as a glaucoma model,[9–11] we sought to develop an ex vivo culture and transduction system based on this species that enables direct observation of the TM and expression of transgenes.

Methods

Feline Immunodeficiency Viral (FIV) Vector Production

A tripartite FIV vector system was used to produce vesicular stomatitis G (VSV-G) pseudotyped lentiviral vectors[12,13] con-

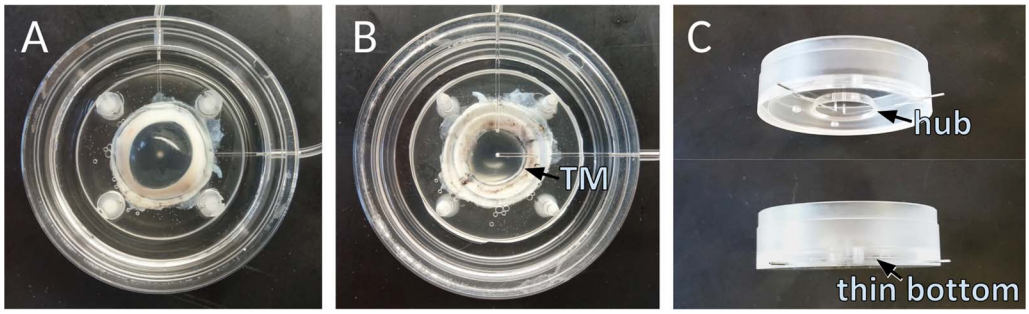

FIGURE 1. Perfused porcine anterior segment culture. (**A**) View of culture dish without cover. (**B**) View through bottom of inverted dish allows the observation of the TM directly with central in-line and peripheral pressure transducer line. (**C**) Side view.

sisting of envelope plasmid pMD.G, packaging plasmid pFP93, and FIV transfer vector GINSIN-encoding enhanced green fluorescent protein (eGFP) and neomycin resistance via an internal ribosomal entry site (IRES).[12]

Lentiviral particles were generated using a new, scaled up transient transfection system with polyethylenimine (PEI) as a polycationic, polymeric transfection agent[14] to provide a simplified and stable platform that allows three full harvests from a single transfection. Prior to transfection, 2.5×10^8 293 T cells that were cycling at a high cell division rate were seeded in a large surface culture vessel (Cell Factory 10; Nunc, Naperville, IL, USA) with 2 L of Dulbecco's modified Eagle's medium (DMEM with 4.5% glucose, 4 mM l-glutamine, without phenol red, without sodium pyruvate; #SH30284.02, Hyclone; GE Healthcare Life Sciences, Piscataway, NJ, USA) at 37°C and supplemented with 10% fetal calf serum and penicillin G sodium/streptomycin sulfate (100 units/mL and 100 μg/mL, Pen Strep, Life Technologies, Grand Island, NY, USA). On the day of transfection (day 0), cell cultures with 80% confluency were incubated with a transfection mix. This transfection mix contained 116 μg of VSV-G envelope plasmid pMD-G, 339 micrograms of packaging plasmid pFP93, and 339 micrograms of transfer plasmid GINSIN which were suspended in 18 mL of 37°C reduced, serum-free media (Opti-MEM; Gibco, Thermo Fisher Scientific, Waltham, MA, USA) that had been combined with 3.2 mL of PEI (polyethylenimine, linear; Polysciences, Inc., Warrington, PA, USA), had been vortexed for 10 seconds, and then allowed to stand for 5 minutes at room temperature. This solution was then pipetted into 1.4 L of fresh media which replaced the one present in the cell factory by gently pouring it along the exchange port without disturbing the cell layers. The cell factory was balanced to distribute the media equally between the layers and placed in an incubator. Following an 8-hour incubation at 37°C, the media containing the transfection mix was replaced with fresh media. Expression of EGFP was imaged by fluorescence microscopy to confirm a transfection rate above 80%. On days 2, 4, and 6, the supernatant was collected and replaced with fresh media. Vector particles were pelleted by ultracentrifugation in a large volume rotor (Type 19; Beckman Coulter Life Sciences, Brea, CA, USA), as previously described,[15,16] and titrated 24 hours later by fluorescence-assisted flow cytometry (FACS) analysis on CrFK cells.[17]

Porcine Eye Anterior Segment Perfusion Culture

Porcine eyes were obtained from the local abattoir and processed within approximately 2 hours of death. The eyelids and adnexal structures were excised, eyes dipped into 5% povidone-iodine ophthalmic solution (betadine 5%; Alcon, Fort Worth, TX, USA) for 30 seconds and then transferred into sterile PBS (Dulbecco's PBS; MP Biomedicals, LLC, Santa Ana, CA, USA). In a tissue culture hood, the eyes were hemisected along the equator followed by removal of the vitreous, lens, ciliary body, iris, retina, and choroid. Pigment shedding was avoided by carefully dissecting the choroid off the sclera directly along the equatorial incision in one piece while leaving the vitreous and lens in place as a barrier toward the anterior chamber. The eyes were irrigated with 10 mL PBS to remove pigment and cellular remnants. The anterior segments were then immediately mounted in perfusion chambers connected to a microinfusion pump (PHD 22/2000; Harvard Apparatus, Holliston, MA, USA) and perfused with serum-free media without phenol red (DMEM with penicillin G sodium/streptomycin sulfate [100 units/mL and 100 μg/mL, respectively]) at a constant flow rate of 3 μL/min. Anterior segments were maintained at 37°C in 5% CO_2. The intraocular pressure was continuously monitored with pressure transducers (physiological pressure transducer, SP844; MEMSCAP, Skoppum, Norway) and recorded using a software system (LabChart; ADInstruments, Colorado Springs, CO, USA). The perfusion system was calibrated using a pressure transducer tester (Veri-Cal; Utah Medical Products, Midvale, UT, USA). Eyes that experienced a contamination, showed erroneous IOP recordings in the negative pressure range, or readings above 30 mm Hg during the first 24 hours were considered a failure. Such negative IOP recordings were observed for instance when debris blocked the transducer lumen while early high IOP was interpreted as relative TM failure or blockage.

Gravity perfused anterior segments (CO_{gr}) were similarly processed and mounted in perfusion chambers connected to a gravity flow system and perfused with serum free clear DMEM supplemented with penicillin G sodium and streptomycin sulfate (100 units/mL and 100 μg/mL, respectively). The gravity flow system utilized a fluid column at a constant height of 20.4 cm above perfusion chambers to maintain pressures at 15 mm Hg. Anterior segments were maintained at 37°C in 5% CO_2.

Transduction

Porcine anterior segments were allowed to stabilize at a constant flow rate for 48 hours before any manipulation. On day 0, the central infusion and transducer lines were disconnected and a bolus of 1 mL of DMEM with 1×10^8 transducing units (TU) GINSIN was injected at a rate of 1mL/min, displacing the same amount of intracameral volume. Both lines were reconnected and constant flow perfusion resumed.

Direct Visualization of the Trabecular Meshwork

We redesigned established anterior chamber perfusion dishes[13,18] by reducing the thickness of the bottom to approximately one-third and widening the now flatter central mounting hub (Fig. 1). Upon upside-down inversion and 30° tilt, the anterior chamber angle could be visualized directly.

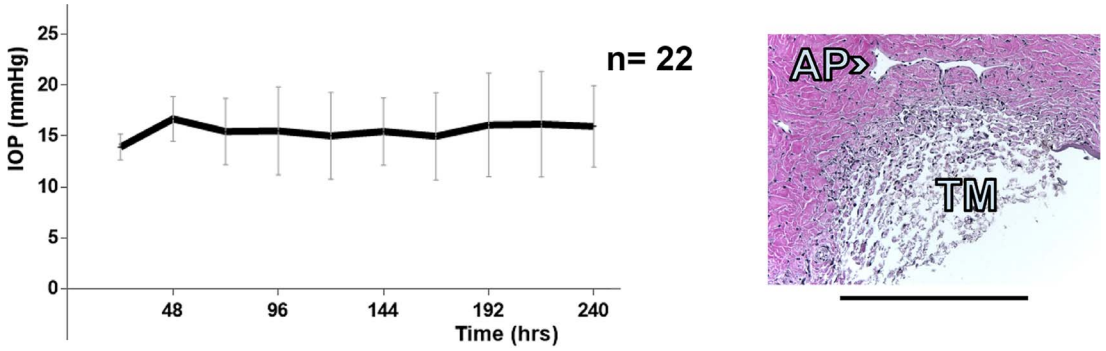

FIGURE 2. Intraocular pressure graph of perfused anterior segment controls ($n = 22$, *left*). Representative histology at the experimental endpoint. AP: aqueous plexus. *Scale bar*: 500 μm.

There was reduced image distortion compared with regular chambers with a thick bottom. On days 1, 3, 7, and 14, anterior segments mounted as described above were inverted and placed under a stereo dissecting microscope equipped for fluorescent imaging (Olympus SZX16 with GFP filter cube and DP80 monochrome/color camera; Olympus Corp., Center Valley, PA, USA) with continued perfusion. The dish was stabilized at a 30° angle and each quadrant was imaged using an exposure of 100 ms, 1360 × 1024 resolution and 8-bit depth. Expression of eGFP was confirmed by identifying single cells by high magnification fluorescence microscopy.

The entire circumference was examined and each quadrant photographed with the dissecting microscope. Fluorescence of TM was graded on a scale of 0 to 4 as previously established: grade 0, no detectable fluorescence; grade 1, single fluorescent spots in the TM; grade 2, numerous, nonconfluent fluorescent spots with some confluent areas; grade 3, extensive, mostly confluent, midlevel transduction; grade 4, extensive, high-level, and confluent fluorescence.[19]

Histology

At the conclusion of the experiment, the anterior segments were removed from the perfusion dish, rinsed in PBS, cut into quadrants, and fixed with 4% paraformaldehyde in PBS for a period of 48 hours before being placed in 70% ethanol. One corneoscleral wedge was taken from each quadrant and paraffin embedded for histologic processing. Paraffin-embedded specimens were cut at 6-μm thickness and stained with hematoxylin eosin (H&E). The ratio of transduced to total TM cells was determined as described previously[19] by counting all TM cells in each of four sections per eye (one from each quadrant). The trabecular meshwork was identified and cell counts of 6-μm H&E-stained paraffin sections obtained for two adjacent quadrants in four transduced and nontransduced anterior segments. Photographs of fluorescent TM were taken of each quadrant at each examination and grades determined in a masked manner using a previously established continuous grading scale.[19]

Statistical Analysis

Total TM cells present in random 6-μm sections from above quadrants were determined by counting the labeled and unlabeled cells and calculating the mean value for each quadrant. An unpaired Student's *t*-test was used for statistical analysis to compare transduced and nontransduced anterior segments. Because of the linear correlation between transduced cells and grades,[19] expression grades were handled as continuous data during the statistical comparison of marker protein accumulation.

RESULTS

Vector production using the scaled up PEI transfection platform yielded 1.1^9 TU total on first, 7.2^8 TU on second and 8.0^8 TU on third harvest with a titer range of approximately 29% at each time point ($n = 3$). Porcine anterior segment cultures experienced a low culture failure rate of 12%. Control anterior segments (Fig. 2) had an IOP of 15.8 ± 1.9 mm Hg during constant perfusion at a rate of 3 μL/min compared with gravity-perfused control anterior segments with an imputed flow rate of 3.7 ± 1.6 μL/min at constant gravity perfusion with a pressure of 15 mm Hg. Control anterior segments were cultured in the redesigned culture system (Fig. 1) and pilot anterior segments kept for up to 21 days during initial viability testing (data not shown). Trabecular meshwork could be observed directly through the bottom of the inverted dishes (Fig. 1) with best detection of eGFP fluorescence when held at a 30° angle (Fig. 3). View was relatively free of distortion for whole eye and quadrant view at up to ×10 magnification but became vertically compressed when viewed at higher magnification or when

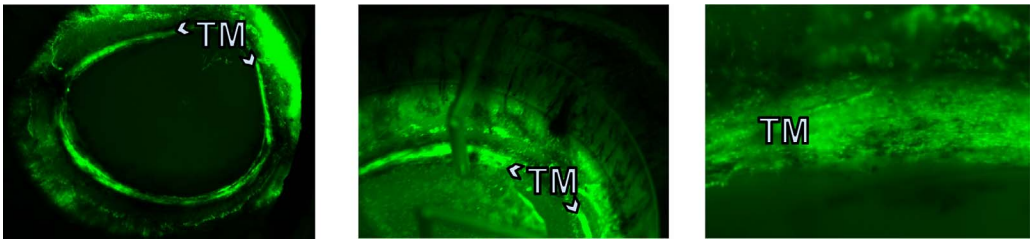

FIGURE 3. Direct, repeated visualization of whole eye with view of transduced TM through the bottom of the redesigned perfusion system. *Left*: Macroscopic view without magnification. *Middle*: Tenfold magnified view of TM. Translucent outflow port with shadow can be seen. *Right*: Fifty-fold magnified view of TM with only minor image distortion (TM is 700 μm wide).

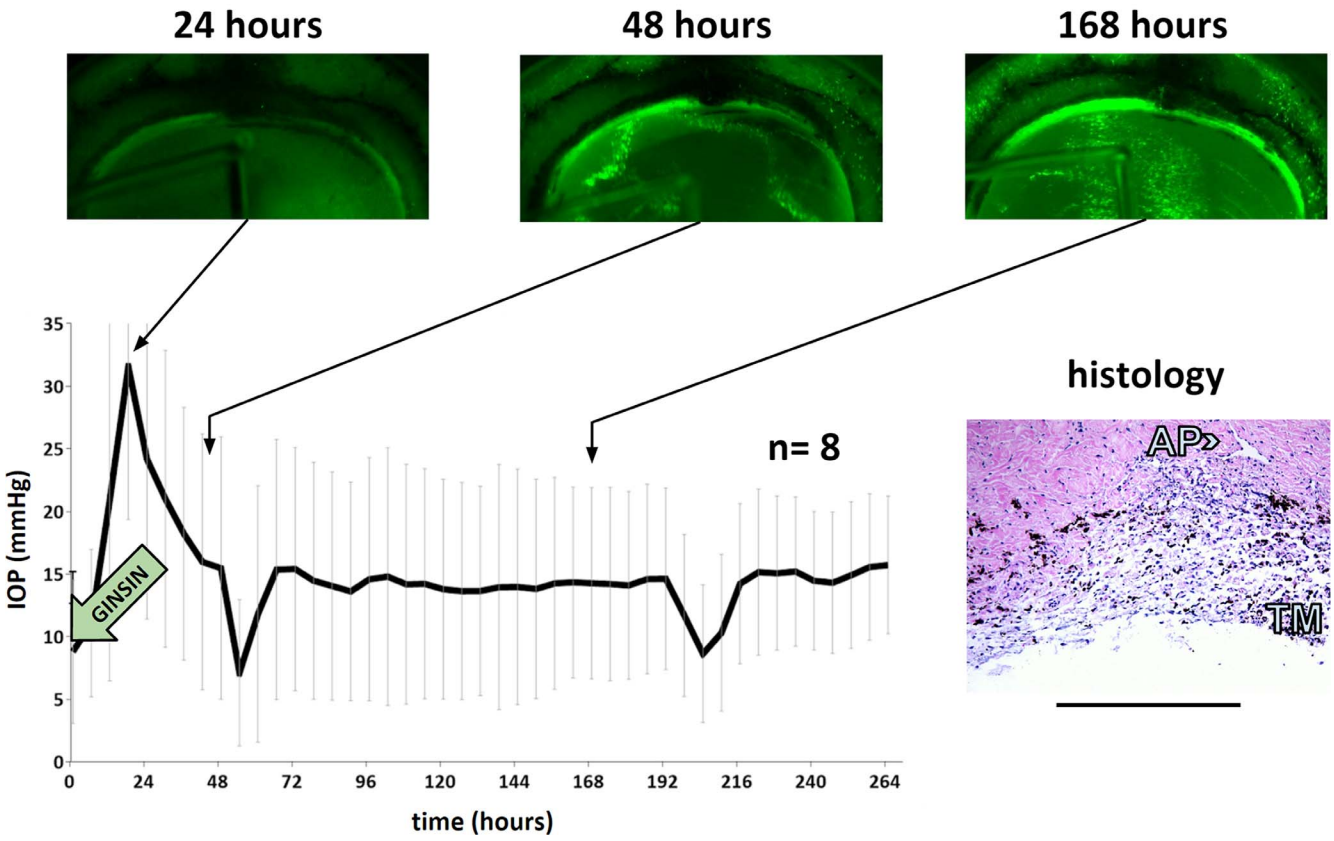

FIGURE 4. Intraocular pressure and directly observed, same eye eGFP expression in TM of eyes transduced with 10^8 TU of eGFP-expressing FIV vector at time points indicated. Intraocular pressure drop at 48 and 192 hours corresponds to perfusion media exchange. Histology was obtained at the experimental endpoint. *Scale bar*: 500 μm.

held at a steeper angle (Fig. 3C). In anterior segments with extensive transduction, fluorescent TM could be seen over 360° but with segmental focus and short areas of non-transduction (Fig. 3). During observation, the eye remained well pressurized and perfused. The most notable IOP changes occurred when the perfusion system was disconnected for media change (Fig. 4).

Within 24 hours of transduction, porcine TM showed low level eGFP marker gene expression after transduction at the highest titer tested, 10^8 TU (Fig. 4). Expression peaked within 48 hours. At this titer, TM transduction was extensive and could be observed throughout the entire periphery. The culture system enabled us to find precise landmarks during serial observation as in the example of the less transduced, more pigmented TM in the center of the fluorescent band of TM in Figure 5 (Fig. 4, identical quadrant of the same eye is shown in time lapse).

Adjacent structures were also occasionally transduced, for instance the sclera (Fig. 3) and corneal endothelium (Fig. 4). Anterior segments of GINSIN transduced with 10^8 TU experienced a significant ($P = 0.03$) but transient posttransduction IOP increase of 44% at 24 hours that resolved at 48 hours (Fig. 4) returning 14.4 ± 2.5 mm Hg without being significantly different from controls. Histology obtained at the conclusion of the experiment indicated a well-preserved TM architecture (Fig. 4, inset).

At transduction with 10^7 TU, no significant IOP elevation occurred (Fig. 5). Instead, these anterior segments experienced a small but significant reduction of IOP ($P = 0.03$) before returning to 14.1 ± 2.4 mm Hg, which was not significantly different from control anterior segments ($P = 0.2$). Expression was initially faint and could only be observed in some anterior segments (Figs. 4, 5) before increasing. At 24 hours, relative GINSIN expression grading in anterior segments transduced with 10^8 TU had an average of 0.5 ± 0.7 ($P < 0.01$) at 24 hours on a scale from 0 to 4 that increased to 2.6 ± 1.1 at 168 hours ($P < 0.01$). Anterior segments transduced with 10^7 TU had a significantly lower expression than those transduced with 10^8 TU. It was 0.2 ± 0.4 at 24 hours which increased to 0.7 ± 1.0 (Fig. 5) at 168 hours. Peaks for both titers were achieved at the same observation time point.

Despite weak or absent fluorescence, the new culture chambers allowed to identify anatomic landmarks in serial observation (Fig. 5, example with same anterior segments and same quadrants). Trabecular meshwork architecture was well preserved in these anterior segments (Fig. 5, inset). Trabecular meshwork cell counts were similar between control and transduced anterior segments (Fig. 6, all $P > 0.6$; Supplementary Fig. S1).

DISCUSSION

There are significant supply challenges for human donor eyes in research which is partially due to the increased rate of corneal endothelium and limbal stem cells transplantation. However, a local abattoir can serve as a source of porcine eyes to produce reliable, high quality anterior segment cultures. Compared with human donor eyes that have a wide age range, disease, and variable time from explantation to culture, the consistency of pig eyes resulted in a considerably lower failure rate in our hands.[13,18] Low costs and close correlation with

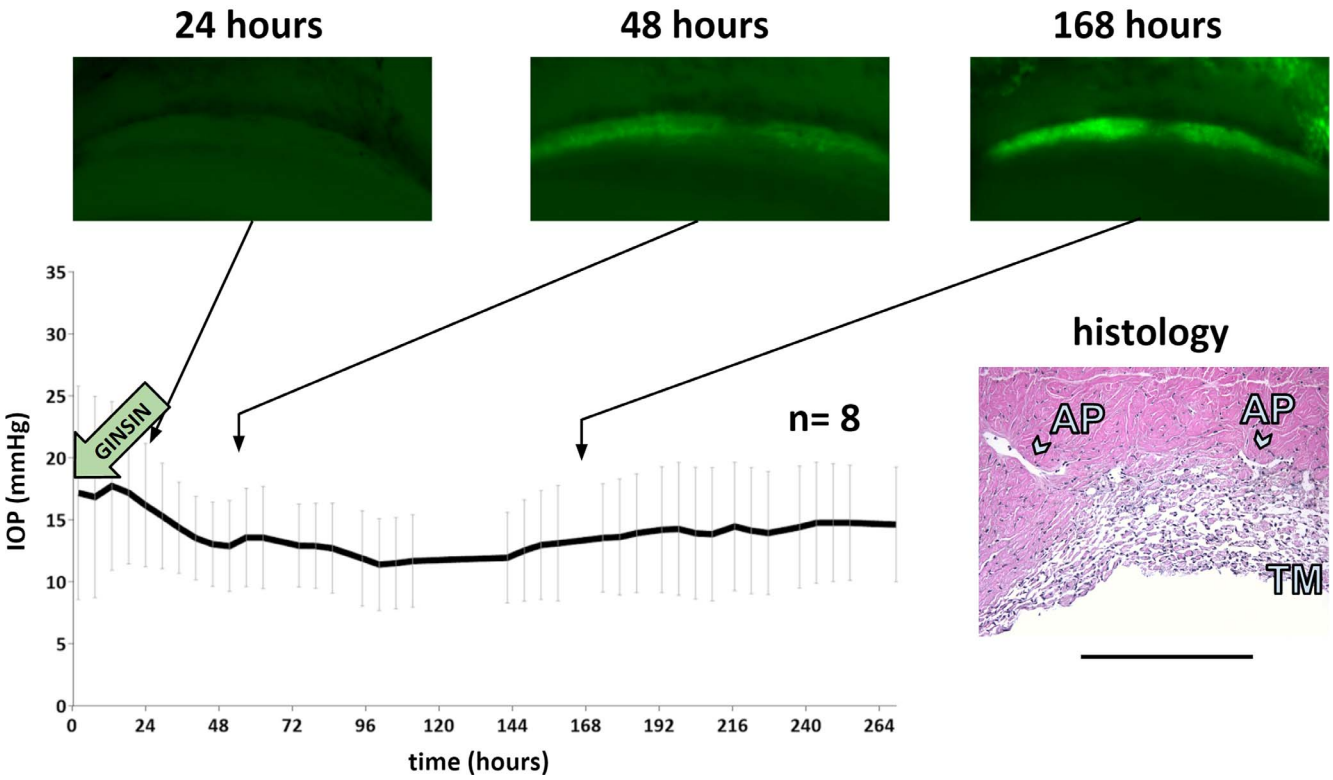

FIGURE 5. Intraocular pressure and directly observed, same eye eGFP expression in TM of eyes transduced with 10^7 TU of eGFP-expressing FIV vector at time points indicated. Gaps in IOP recording at 72 and 120 hours correspond to perfusion media exchange. Histology was obtained at the experimental endpoint. *Scale bar*: 500 μm.

human anatomy make pig eyes an attractive model for research[20,21] and training in ophthalmology.[22,23] The pig's similarity in size and anatomy also led to research into xenotransplantation with a focus on kidney, liver, and cornea[24] and, more recently, the outflow tract.[10]

Here, we describe a method to track transgene expression in an ex vivo pig eye culture system by direct observation that is made possible by redesigned, thinner culture dishes. The ability to directly observe the TM from the inside will provide a valuable tool to correlate expression of transgenes in the TM with the resulting segmental outflow changes as measured in quantitative canalograms obtained from the outside (Loewen R, et al. *IOVS* 2015;56:ARVO E-Abstract 2225846).

The intraocular pressure of 15.8 ± 1.9 mm Hg we observed at the normal aqueous flow rate of 3 to 4 μL/min[21,25] is close to the physiologic IOP of 15.2 ± 1.8 mm Hg[26] of pigs and has been used in other porcine ex vivo studies.[27,28] This intraocular pressure, obtained with a perfusion rate of 3 μL/min, matches our imputed outflow of 3.7 ± 1.6 μL/min using the reverse approach of infusing these eyes at 15 mm Hg in our constant pressure experiments.[29] In contrast to these studies, we did not observe any prominent corneal swelling that can occur without a physiological transcorneal pressure gradient that allows proper nutrient transport into the stroma[30] and preservation of normal corneal thickness and contour.[31,32] The short time from enucleation to culture and limited exposure to povidone-iodine may have further reduced corneal compromise.

Problems encountered in prior use of pig eyes include pigment release resulting in trabecular meshwork obstruc-

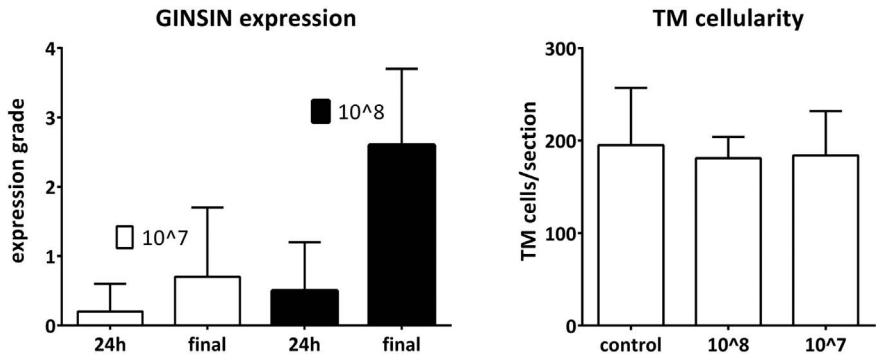

FIGURE 6. Expression grades of eyes transduced with 10^7 and 10^8 TU (*left*, $n = 8$ for each group; *error bars* = SD) and corresponding TM cellularity (*right*, $n = 8$ eyes for each group with two sections per eye counted from adjacent quadrants; *error bars* ± SD).

tion,[21] the larger diameter that not all human eye culture systems can accommodate, and the more plexus-like, discontinuous segments of Schlemm's canal.[5] The discontinuity of Schlemm's canal may be an advantage for new outflow research strategies concerned with focal TM modification by limiting effects to the immediate downstream drainage system and providing the opportunity for localized flow measurements. Segmental flow has recently been observed in other species as well.[33,34] By dissecting the choroid off the sclera directly along the equatorial incision and using the lens as a barrier toward the anterior chamber, we avoided the complexity of prior protocols meant to reduce pigment shedding.[21] Copious irrigation alone was not sufficient to dislodge pigment that had already made it into the TM.

We developed a protocol for scaled-up FIV vector production with PEI transfection that provided reliable high titers eliminating the pH and titer variability of traditional production systems using calcium chloride.[35] Because transfected cell layers remained adherent, the vector could be harvested three times for an entire week with only moderate decline of titers. Feline immunodeficiency virus, a nonprimate lentiviral vector that has the safety advantage of not being based on a human pathogen, can transduce primate,[13,18,36] feline,[2,19] and rodent[12] trabecular meshwork at a high level. This observation was principally the same in pig eyes, including a limited and temporary effect on outflow function at the highest titers.[13] Different from prior species, the corneal endothelium and sclera that were in proximity to the TM in pig eyes appeared to be transduced more often. This could be caused by different flow kinetics due to a relatively large anterior chamber with a less selective contact and perfusion of the target tissue. This vector does not currently deploy receptor or transcriptional targeting strategies that may become necessary in cytoablative models.[12] The somewhat lower expression levels compared with human[13] and feline[19] eyes may indicate that lentiviral restriction is present but can be overcome at higher titers. Defense mechanisms to curb lateral intrusion of foreign code from retro-elements are known in many species and the most important restriction factors found in human cells are also present in the pig as a genome search for APOBEC-3F,[37] TRIM5,[38] BST2,[39] SAMHD1,[40] and ZAP[41] demonstrates. Restriction has not presented an obstacle to lentiviral germline transgenesis with HIV and EIAV vectors[42–45] and should not impede future use of these vectors in anterior segments. Relevant to biosafety in TM engineering studies involving xenotransplantation, the pig genome harbors porcine endogenous retroviruses (PERV-A, -B, and -C),[46,47] but these encounter TRIM[48] and APOBEC3[49]-mediated restriction in human cells.

In conclusion, we found that pig eyes can be used as a reliable and high quality source for anterior segment perfusion cultures. The trabecular meshwork could be transduced and expression monitored serially. The ability to manipulate and directly observe the TM in this culture system, combined with the relative similarity to human eyes, will provide useful tools for new approaches of bioengineering in glaucoma research.[10,50]

Acknowledgments

Supported by Grant K08EY022737 (NAL); the American Glaucoma Society (NAL); Grant P30-EY08099 (JSS); Grant EY021727 (MPF); and Research to Prevent Blindness (JSS, MPF)

Disclosure: **R.T. Loewen**, None; **P. Roy**, None; **D.B. Park**, None; **A. Jensen**, None; **G. Scott**, None; **D. Cohen-Karni**, None; **M.P. Fautsch**, None; **J.S. Schuman**, None; **N.A. Loewen**, None

References

1. Bramley T, Peeples P, Walt JG, Juhasz M, Hansen JE. Impact of vision loss on costs and outcomes in Medicare beneficiaries with glaucoma. *Arch Ophthalmol*. 2008;126:849–856.
2. Khare PD, Loewen N, Teo W, et al. Durable, safe, multi-gene lentiviral vector expression in feline trabecular meshwork. *Mol Ther*. 2008;16:97–106.
3. McMenamin PG, Steptoe RJ. Normal anatomy of the aqueous humour outflow system in the domestic pig eye. *J Anat*. 1991; 178:65–77.
4. Suárez T, Vecino E. Expression of endothelial leukocyte adhesion molecule 1 in the aqueous outflow pathway of porcine eyes with induced glaucoma. *Mol Vis*. 2006;12:1467–1472.
5. Tripathi RC. Ultrastructure of the exit pathway of the aqueous in lower mammals: (a preliminary report on the "angular aqueous plexus"). *Exp Eye Res*. 1971;12:311–314.
6. Groenen MAM, Archibald AL, Uenishi H, et al. Analyses of pig genomes provide insight into porcine demography and evolution. *Nature*. 2012;491:393–398.
7. Flicek P, Amode MR, Barrell D, et al. Ensembl 2014. *Nucleic Acids Res*. 2014;42:D749–D755.
8. Pairwise alignment human vs pig LastZ results. Ensembl. Available at: http://useast.ensembl.org/info/genome/compara/mlss.html?mlss=716. Accessed August 17, 2015.
9. Lei Y, Stamer WD, Wu J, Sun X. Endothelial nitric oxide synthase-related mechanotransduction changes in aged porcine angular aqueous plexus cells. *Invest Ophthalmol Vis Sci*. 2014;55:8402–8408.
10. Abu-Hassan DW, Li X, Ryan EI, Acott TS, Kelley MJ. Induced pluripotent stem cells restore function in a human cell loss model of open-angle glaucoma. *Stem Cells*. 2015;33:751–761.
11. Li N, Shi H-M, Cong L, Lu Z-Z, Ye W, Zhang Y-Y. Outflow facility efficacy of five drugs in enucleated porcine eyes by a method of constant-pressure perfusion. *Int J Clin Exp Med*. 2015;8: 7184–7191.
12. Zhang Z, Dhaliwal AS, Tseng H, et al. Outflow tract ablation using a conditionally cytotoxic feline immunodeficiency viral vector. *Invest Ophthalmol Vis Sci*. 2014;55:935–940.
13. Loewen N, Bahler C, Teo WL, et al. Preservation of aqueous outflow facility after second-generation FIV vector-mediated expression of marker genes in anterior segments of human eyes. *Invest Ophthalmol Vis Sci*. 2002;43:3686–3690.
14. Ehrhardt C, Schmolke M, Matzke A, et al. Polyethylenimine, a cost-effective transfection reagent. *Signal Transduct*. 2006;6: 179–184.
15. Loewen N, Barraza R, Whitwam T, Saenz DT, Kemler I, Poeschla EM. FIV vectors. *Methods Mol Biol*. 2003;229:251–271.
16. Saenz DT, Barraza R, Loewen N, Teo W, Poeschla EM. Production and harvest of feline immunodeficiency virus-based lentiviral vector from cells grown in T75 tissue-culture flasks. *Cold Spring Harb Protoc*. 2012;2012:124–125.
17. Saenz DT, Barraza R, Loewen N, Teo W, Poeschla EM. Titration of feline immunodeficiency virus-based lentiviral vector preparations. *Cold Spring Harb Protoc*. 2012;2012:126–128.
18. Loewen N, Fautsch MP, Peretz M, et al. Genetic modification of human trabecular meshwork with lentiviral vectors. *Hum Gene Ther*. 2001;12:2109–2119.
19. Loewen N, Fautsch MP, Teo W-L, Bahler CK, Johnson DH, Poeschla EM. Long-term, targeted genetic modification of the aqueous humor outflow tract coupled with noninvasive imaging of gene expression in vivo. *Invest Ophthalmol Vis Sci*. 2004;45:3091–3098.
20. Lei Y, Overby DR, Read AT, Stamer WD, Ethier CR. A new method for selection of angular aqueous plexus cells from

porcine eyes: a model for Schlemm's canal endothelium. *Invest Ophthalmol Vis Sci*. 2010;51:5744–5750.

21. Bachmann B, Birke M, Kook D, Eichhorn M, Lütjen-Drecoll E. Ultrastructural and biochemical evaluation of the porcine anterior chamber perfusion model. *Invest Ophthalmol Vis Sci*. 2006;47:2011–2020.
22. van Vreeswijk H, Pameyer JH. Inducing cataract in postmortem pig eyes for cataract surgery training purposes. *J Cataract Refract Surg*. 1998;24:17–18.
23. Lee GA, Chiang M, Shah P. Pig eye trabeculectomy—a wet-lab teaching model. *Eye (Lond)*. 2005;20:32–37.
24. Ekser B, Ezzelarab M, Hara H, et al. Clinical xenotransplantation: the next medical revolution? *Lancet*. 2012;379:672–683.
25. Wagner JA, Edwards A, Schuman JS. Characterization of uveoscleral outflow in enucleated porcine eyes perfused under constant pressure. *Invest Ophthalmol Vis Sci*. 2004; 45:3203–3206.
26. Ruiz-Ederra J, García M, Hernández M, et al. The pig eye as a novel model of glaucoma. *Exp Eye Res*. 2005;81:561–569.
27. Borrás T, Rowlette LL, Erzurum SC, Epstein DL. Adenoviral reporter gene transfer to the human trabecular meshwork does not alter aqueous humor outflow. Relevance for potential gene therapy of glaucoma. *Gene Ther*. 1999;6:515–524.
28. Sanchez I, Martin R, Ussa F, Fernandez-Bueno I. The parameters of the porcine eyeball. *Graefes Arch Clin Exp Ophthalmol*. 2011;249:475–482.
29. Keller KE, Bradley JM, Vranka JA, Acott TS. Segmental versican expression in the trabecular meshwork and involvement in outflow facility. *Invest Ophthalmol Vis Sci*. 2011;52:5049–5057.
30. Thiel MA, Morlet N, Schulz D, et al. A simple corneal perfusion chamber for drug penetration and toxicity studies. *Br J Ophthalmol*. 2001;85:450–453.
31. Pierscionek BK, Asejczyk-Widlicka M, Schachar RA. The effect of changing intraocular pressure on the corneal and scleral curvatures in the fresh porcine eye. *Br J Ophthalmol*. 2007; 91(6):801–803.
32. Kling S, Marcos S. Contributing factors to corneal deformation in air puff measurements corneal deformation in air puff measurements. *Invest Ophthalmol Vis Sci*. 2013;54:5078–5085.
33. Vranka JA, Bradley JM, Yang Y-F, Keller KE, Acott TS. Mapping molecular differences and extracellular matrix gene expression in segmental outflow pathways of the human ocular trabecular meshwork. *PLoS One*. 2015;10:e0122483.
34. Swaminathan SS, Oh DJ, Kang MH, Rhee DJ. Aqueous outflow: segmental and distal flow. *J Cataract Refract Surg*. 2014;40: 1263–1272.
35. Saenz DT, Barraza R, Loewen N, Teo W, Poeschla EM. Production, harvest, and concentration of feline immunodeficiency virus-based lentiviral vector from cells grown in CF10 or CF2 devices. *Cold Spring Harb Protoc*. 2012;2012:118–123.
36. Barraza RA, Rasmussen CA, Loewen N, et al. Prolonged transgene expression with lentiviral vectors in the aqueous humor outflow pathway of nonhuman primates. *Hum Gene Ther*. 2009;20:191–200.
37. DNA dC->dU-editing enzyme APOBEC-3F [Sus scrofa]. National Center for Biotechnology Information (NCBI). Bethesda, MD: National Library of Medicine. http://www.ncbi.nlm.nih.gov/protein/147905488?report=genbank&log$=prottop&blast_rank=1&RID=W21DDYBJ01R. Accessed August 4, 2015.
38. Tripartite motif protein TRIM5 [Sus scrofa]. NCBI. Bethesda, MD: National Library of Medicine. Available at: http://www.ncbi.nlm.nih.gov/protein/NP_001037997.1. Accessed August 4, 2015.
39. Bone marrow stromal antigen 2 [Sus scrofa]. NCBI. Bethesda, MD: National Library of Medicine. Available at: http://www.ncbi.nlm.nih.gov/protein/NP_001155227.1. Accessed August 4, 2015.
40. Deoxynucleoside triphosphate triphosphohydrolase SAMHD1-like [Sus scrofa]. NCBI. Bethesda, MD: National Library of Medicine. Available at: http://www.ncbi.nlm.nih.gov/protein/NP_001279034.1. Accessed August 4, 2015.
41. Zinc finger CCCH-type antiviral protein 1 [Sus scrofa]. NCBI. Bethesda, MD: National Library of Medicine. Available at: http://www.ncbi.nlm.nih.gov/protein/NP_001170960.1. Accessed August 4, 2015.
42. Renner S, Fehlings C, Herbach N, et al. Glucose intolerance and reduced proliferation of pancreatic beta-cells in transgenic pigs with impaired glucose-dependent insulinotropic polypeptide function. *Diabetes*. 2010;59:1228–1238.
43. Baxa M, Hruska-Plochan M, Juhas S, et al. A transgenic minipig model of Huntington's disease. *J Huntingtons Dis*. 2013;2:47–68.
44. Kostic C, Lillico SG, Crippa SV, et al. Rapid cohort generation and analysis of disease spectrum of large animal model of cone dystrophy. *PLoS One*. 2013;8:e71363.
45. Whitelaw CBA, Radcliffe PA, Ritchie WA, et al. Efficient generation of transgenic pigs using equine infectious anaemia virus (EIAV) derived vector. *FEBS Lett*. 2004;571:233–236.
46. Takeuchi Y, Patience C, Magre S, et al. Host range and interference studies of three classes of pig endogenous retrovirus. *J Virol*. 1998;72:9986–9991.
47. Moalic Y, Blanchard Y, Félix H, Jestin A. Porcine endogenous retrovirus integration sites in the human genome: features in common with those of murine leukemia virus. *J Virol*. 2006; 80:10980–10988.
48. Mazurek U, Kimsa MW, Strzalka-Mrozik B, et al. Microarray analysis of retroviral restriction factor gene expression in response to porcine endogenous retrovirus infection. *Pol J Microbiol*. 2014;63:183–190.
49. Park SH, Kim JH, Jung YT. Differential sensitivity of porcine endogenous retrovirus to APOBEC3-mediated inhibition. *Arch Virol*. May 2015;160:1901–1908.
50. Du Y, Yun H, Yang E, Schuman JS. Stem cells from trabecular meshwork home to TM tissue in vivo. *Invest Ophthalmol Vis Sci*. 2013;54:1450–1459.

Investigative Ophthalmology & Visual Science